




Crystal growth and properties of pure L-alanine and boric acid doped L-alanine nonlinear optical single crystals for frequency conversion

A. Dilli Rani¹, C. Rathika Thaya Kumari², M. Nageshwari², P. Sangeetha¹, G. Vinita³, M. Lydia Caroline^{4,*} , and S. Kumaresan¹

¹PG and Research Department of Physics, Arignar Anna Government Arts College, Cheyyar 604407, Tamilnadu, India

²Department of Physics, Bharath Institute of Higher Education and Research, Chennai 600073, India

³Division of Physics, School of Advanced Science, VIT University, Chennai 600 127, India

⁴Department of Physics, Dr Ambedkar Govt Arts College, Vyasarpadi, Chennai 600 039, India

Received: 18 September 2022

Accepted: 12 December 2022

Published online:
25 January 2023

© The Author(s), under exclusive licence to Springer Science+Business Media, LLC, part of Springer Nature 2023

ABSTRACT

Frequency conversion materials such as pure and 5 wt % Boric acid doped L-alanine crystals are grown using the slow evaporation technique at room temperature. Single crystal XRD reported that the crystals formed attained the orthorhombic system of noncentrosymmetric space group $P2_12_12_1$. FTIR analysis established the presence of groups such as COO^- , NH_3^+ , CH_2 , CH and boron (B) element from shift in vibrational modes of at lower frequency region is also confirmed by EDAX measurement. The UV-Vis spectral study predicted the cut-off wavelength for pure LA and boric acid doped LA at 245 nm and 238 nm and thereby energy gap, Urbach energy were also evaluated. Vicker's micro-hardness study categorized the harvested crystals as soft materials following RISE effect. The dielectric characterization such as dielectric constant and dielectric loss were studied at various temperature ranges. Jonscher's power law verifies the conductivity mechanism with $s = 0.988, 0.985$ for pure LA and doped LA. Laser damage threshold study using an Nd:YAG laser (1064 nm) evinces the stability of the material to withstand high intensity lasers in NLO applications. The luminescence nature of crystals was investigated in the range 250–600 nm and confirmed violet emission radiation. TGA-DTA analysis showed that the crystals possess good thermal stability. Second harmonic generation (SHG) was examined from the emission of green light from the samples by Kurtz Perry technique. The Z-scan investigations on the crystals reveal that they undergo two photon absorption, self-defocusing and hence greater third order nonlinear susceptibility χ^3 of order of 10^{-8} esu encompasses the grown crystals in the development of opto-electronic devices and for the conversion of energy process.

Address correspondence to E-mail: lydiacaroline2006@yahoo.co.in

1 Introduction

Focussing on the growth of nonlinear optical (NLO) crystals helps in designing of materials in the domain of optoelectronics and photonics. NLO crystals exhibiting frequency conversion efficiency such as second harmonic generation (SHG) and third harmonic generation (THG) have a greater impact in photonic industry [1]. In distinct class of materials of non-polar benzyl group NLO chromophore, nonlinear optical effects exhibiting noncentrosymmetric phenomena have perceived at relatively large intensities [2]. Crystals of organic category possessing flexibility of molecules, and structural diversity allow fine tuning of the chemical structures and thus gaining optical nonlinearities and ultra-fast response times and tunable electro-optic filters [3, 4]. Enormous organic materials has been investigated in the previous times such as LAA, LPDMA, LAPA by Sangeetha et al., Jayaprakash et al., Jothimani et al. [5–7] declares the materials versatility in opto-electronics field occupying wide space signal processing and photonic switching devices, owing to their strong nonlinear optical absorption enabling optical limiting property. Frequency doubling phenomenon, a visibly dramatic nature was observed among the various nonlinear optical procedures such as frequency doublers, optical imaging, electro-optic modulators, high resolution printing and spectroscopy [8]. Also considering the organic molecular chiral level, the shift in the transfer of charge is supposed to control the output of SHG at the same time on the supramolecular level demands high output of SHG towards strong noncentrosymmetric molecular interaction and superior phase matching stability [9, 10].

The frequency tripling effect or THG examined using Z-scan technique greatly occupies future specific applications in optoelectronics and photonics [11]. Recent work on nonlinear optical crystals proved that organic molecules exposed wide range of third-order sensitivity paved a way to devise optoelectronic and photonics [5, 6, 10].

The role of organic crystals in nonlinear optics (NLO) applications due to their high nonlinear susceptibility [8] possessing delocalized electrons is of great interest. Amongst the organic crystals, aminoacids show specific features of interest such as molecular chirality, absence of strongly conjugated bonds, leading to wide transparency ranges in the

visible and UV spectral regions, zwitterionic nature of molecules which creates hydrogen bond networks and chiral auxiliaries for nitro-aromatics and other donor–acceptor molecules having π electronic configuration with large hyperpolarizabilities and also as a basis for synthesizing organic–inorganic compounds [12–14].

Our work discloses the progress of growth and characterization of smallest aminoacid L-alanine and 5 wt % of boric acid doped L-alanine nonlinear optical single crystals grown from low temperature solution growth process ensure a new focus of science and development of techniques in photonics. Individually the study on L-alanine has been studied by many authors and also structure refinement has been reported [7, 8, 15–18]. L-Alanine (LA) exhibit noncentrosymmetric nature with a methyl group ($-\text{CH}_3$) as side chain [8].

Many researchers have worked on borate-based crystals [19, 20] including Caroline et al. and Rathika et al. [21, 22] have reported metal doped with aminoacid L-alanine suitable for direct conversion process between electrons and photons such as optical computing, optical communication, optical data storage and electro-optic modulators. Boric acid $\text{B}(\text{OH})_3$ also named as boric acid, orthoboric acid, borofax was structurally determined by Zachariason [23] from X-ray measurement. Later Bernal and Megaw studied the bonding of hydrogen atoms which was confirmed experimentally by Cowley [24]. Borate incorporated materials occupy a key place in frequency conversion as a tunable laser source in UV region [25]. The various studies on structure of boric acid $\text{B}(\text{OH})_3$ and infrared spectrum has been reported [24, 26]. Due to unique physical properties of borates like high damage threshold, high optical quality, showing wide range of transparency in UV region, large efficient nonlinear coefficient and luminescence comes under basic characteristics of borates leading to serve as unique materials in the domain of laser including short wavelength laser techniques [27–30]. Herein, we report synthesis of L-alanine and boric acid doped L-alanine utilizing the process of slow evaporation and obtained crystals were subjected to various characterizations namely dielectric, mechanical, thermal, fluorescence, Laser Damage Threshold, SEM and EDAX, second- and third-order nonlinearity in addition to the linear optical characteristics of the grown crystals.

2 Experimental process

2.1 Crystal growth

The pure L-alanine and 5 wt % Boric acid doped L-alanine crystals are grown using water as solvent by slow evaporation technique. From the knowledge of solubility of 19.0 g/100 ml for pure L-alanine at 45 °C in water and boric acid with a water solubility 50 g/litre at 50 °C [26], pure L-alanine and boric acid ($B(OH)_3$) with 5 wt % doped with LA were taken in different vessels to prepare saturated solution. Both pure and boric acid doped LA was separately stirred for 7 h using magnetic stirrer at room temperature. The obtained homogenous state of saturated solutions were kept in petri dishes for slow evaporation to take place. The transparent crystals of LA and boron presence LA were harvested in growth duration of 15–20 days. The pictures of LA and boron element doped LA are presented in Fig. 1(a, b).

3 Results and discussion

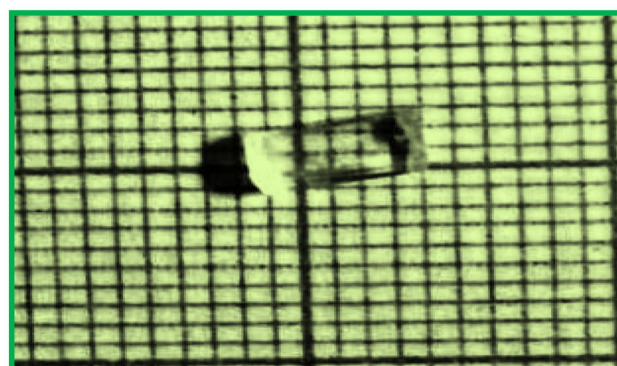
3.1 Single crystal XRD studies (SXR)

The grown-up crystals were investigated by BRUKER APPA APEX II CCD diffractometer. The study discloses the orthorhombic crystal structure with unit cell parameters $a = 6.032 \text{ \AA}$, $b = 12.343 \text{ \AA}$, $c = 5.784 \text{ \AA}$, $V = 428.9 \text{ \AA}^3$, $\alpha = \beta = \gamma = 90^\circ$ for LA and $a = 6.01 \text{ \AA}$, $b = 12.3 \text{ \AA}$, $c = 5.77 \text{ \AA}$, $\alpha = \beta = \gamma = 90^\circ$ for boric acid doped L-alanine which attained the same crystal system of the parent LA with $P2_12_12_1$ noncentrosymmetric space group [8].

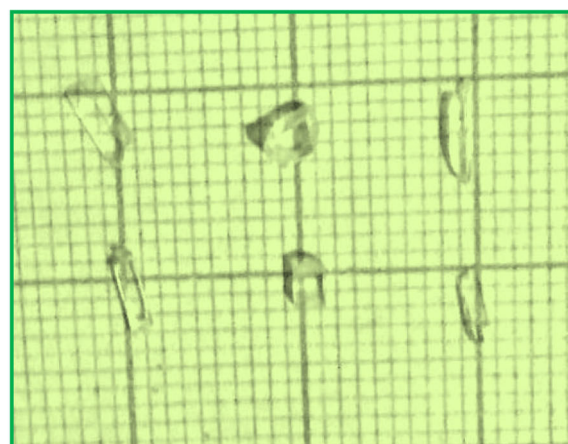
3.2 FT-IR Vibrational Study

In the recorded FTIR spectroscopy, the characteristic absorption spectra for the various functional groups present in the parent LA (Fig. 2a) agree well with the FTIR spectra studied in the literature [8] and BA doped LA crystal FTIR profile (Fig. 2b), shows certain shift in the wavenumbers confirming the presence of boron and zwitterion in both crystals.

The occurrence of fundamental vibrational modes due to COO^- , NH_3^+ , CH_2 , CH groups are noticed in parent LA and doped LA. The carboxylic group is seen to exist as COO^- in both the crystals with the characteristic vibrations seen in the range



a. Picture of L-alanine (LA)



b. Photograph of boric acid doped LA

Fig. 1 a. Picture of L-alanine (LA). b. Photograph of boric acid mixed LA

1680–1540 cm^{-1} due to strong asymmetric stretching, i.e. at 1451 cm^{-1} (LA) and at 1441 cm^{-1} (BA doped LA), weak symmetric stretching observed at 1414 cm^{-1} (LA) and at 1410 cm^{-1} (BA doped LA) and scissoring mode is seen in the profiles pertaining to wavenumbers positioned at 644 cm^{-1} (LA) and 643 cm^{-1} (BA doped LA), respectively.

The ionization of the carboxyl group is confirmed from the IR bands observed at 539 cm^{-1} , 530 cm^{-1} and 1414 cm^{-1} , 1410 cm^{-1} in LA and doped LA spectra. The presence of NH_3^+ group in aminoacids, the stretching and bending vibrational modes are usually expected in the regions 3150–3000 cm^{-1} , 1660–1650 cm^{-1} and 1550–1480 cm^{-1} .

In the recorded FTIR profiles (Fig. 2a and b), the IR bands existed at the positions 3081 cm^{-1} and 3048 cm^{-1} , 1617 cm^{-1} and 1624 cm^{-1} is a clear indication for the presence of NH_3^+ group in the grown crystals, denoting the participation of three hydrogen atoms in the hydrogen bonding thereby weakening

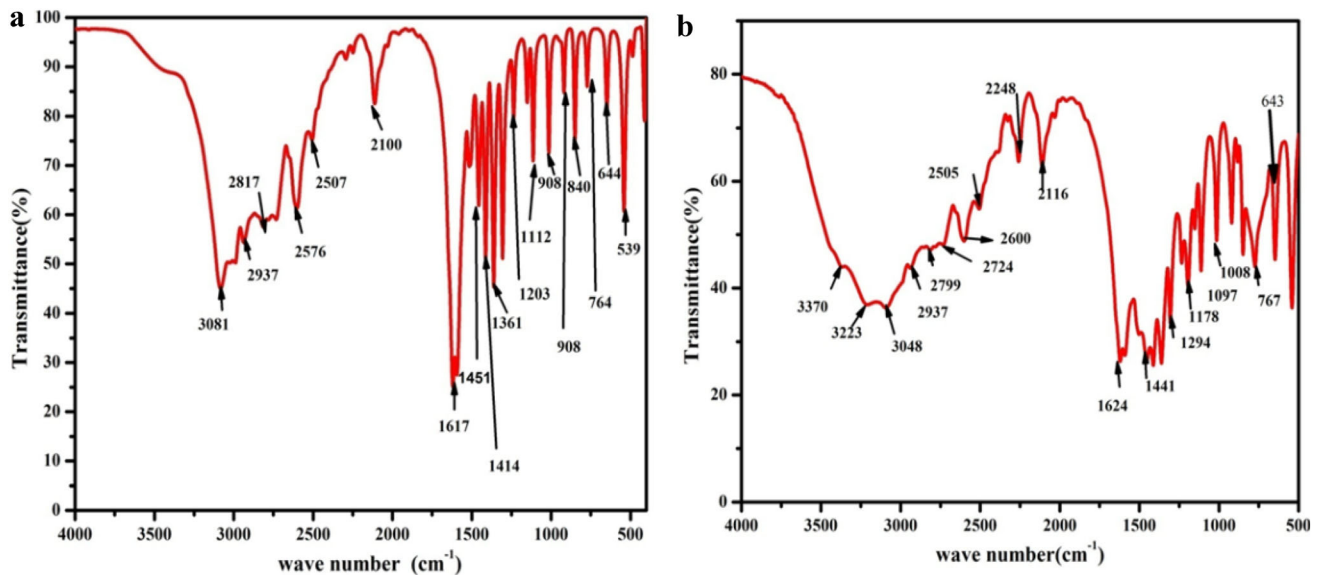


Fig. 2 (a,b) FTIR Spectrum of LA and Boric Acid doped LA

the N–H bond [8]. The vibrational modes observed just below 3000 cm^{-1} are weakly resolved due to methyl and methane groups. The absorption bands for C–N and C–C stretching vibrations are noticed in the wavenumber region $850\text{--}1150\text{ cm}^{-1}$ for the studied crystals. The wavenumber seen at around 840 cm^{-1} and at 838 cm^{-1} in the recorded FTIR profile for parent and doped crystals, are assigned to C–N symmetric stretching vibration.

The presence of Boron element in the doped LA crystal can be attributed to the wavenumbers between $800\text{--}600\text{ cm}^{-1}$ [25]. The IR bands at 1097 cm^{-1} corresponds to C–C stretching. The shift in the wavenumbers observed in Fig. 2b compared to Fig. 2a clarifies the incorporation of boron in L-alanine, the same being ascertained from the wavelength at low frequency region [31] and hence supported from EDAX analysis. Henceforth in both crystals, the zwitterion structure of amino acids comprising of NH_3^+ group acts as a good hydrogen bond donor and carboxylic group as an excellent acceptor confirmed by strong hydrogen bonds between them in the crystal lattice of LA and BA doped LA. The characteristic vibrational frequencies of obtained pure LA and BA doped LA shows shift in the peaks is presented in Table 1.

3.3 UV–Visible analysis

In the domain of optical field, materials having excellent transmittance are needed [32]. The UV–

Visible study of LA and boric acid doped LA crystals reveal high transmittance in the entire visible region. The spectra were recorded using LAMBDA-35 UV–Visible spectrophotometer Fig. 3(a, b). The lower cut off wavelength was observed at 245 nm (LA) and 238 nm (BA doped LA) reveal that they could occupy an important place in generation of blue/violet light using a diode laser [32]. The spectra aims to give structural information since absorption of UV and visible light involves rising of electrons in π and n orbital from ground state to excited state through the photon absorption process [33].

3.3.1 Calculation of Band gap

The optical energy gap (E_g) of the material provides useful information regarding the band structure of electronic states of crystals [34]. The band gap was calculated by,

$$\alpha hv = A(hv - E_g)^{1/2} \quad (1)$$

Here, h (Planck's constant), ν (frequency), A (constant). The energy gap of the material was estimated by Tauc's graph plotted between $(\alpha hv)^2$ versus $h\nu$ (Fig. 4a, b). The calculated wide band gap of 5.34 eV (LA) and 5.31 eV (doped LA) suggest enormous transmittance in visible range creates the crystals suitability in the sector of nonlinear optics includes optoelectronic devices.

Table 1 Assignments of vibrational frequencies observed in IR spectra of pure LA and BA doped LA

Present work (pure LA) IR (cm ⁻¹)	Present work (BA doped LA) IR (cm ⁻¹)	Assignments
3442	3370	OH stretching vibrations
3250	3223	N-H stretching
3081	3048	NH ₃ ⁺ symmetric stretching
2937	2937	CH ₂ asymmetric stretching
2817	2799	CH stretching in CH ₃
2100	2116	Combination band of NH ₃ ⁺ degenerate mode and of NH ₃ ⁺ torsion
1617,1600	1624	NH ₃ ⁺ asymmetric stretching
1451	1441	symmetric stretching of COO ⁻
1414	1410	symmetric stretching of COO ⁻
1361	1371	NH ₂ scissoring and bending
1172	1178	Rocking modes of NH ₃
1112	1097	C-C stretch
840	838	C-C-N symmetric stretching vibration
764	767	O-C-O bending mode
644	643	Symmetric deformation of COO ⁻
539	530	Ionization of carboxyl group

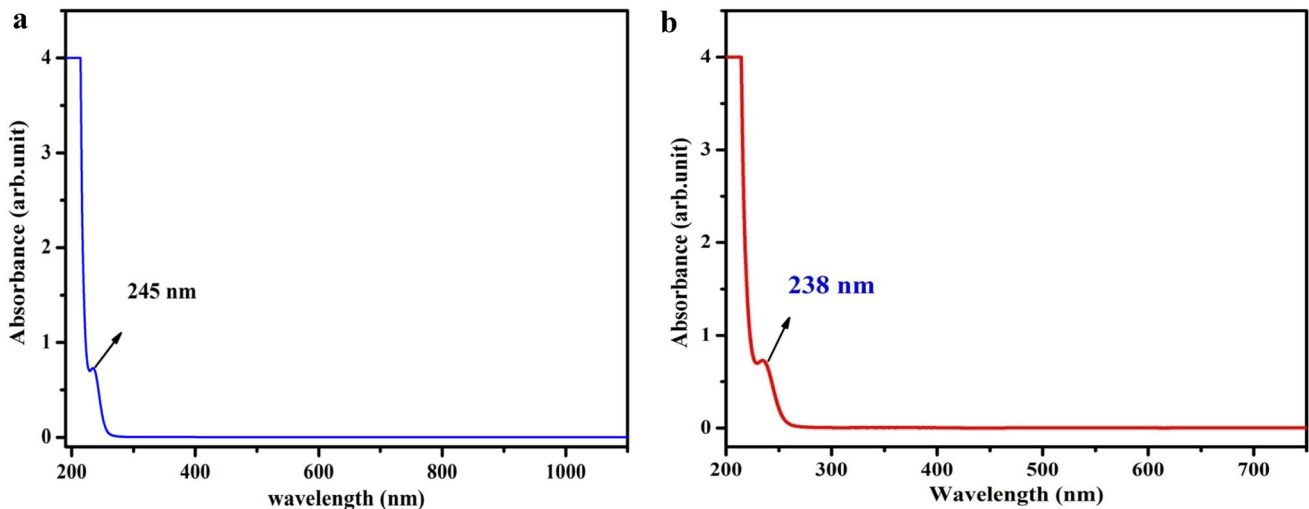


Fig. 3 (a, b). UV-Vis spectra of LA and boric acid doped LA

3.3.2 Urbach's energy

The presence of absorption coefficient value in close proximity to the band edge shows an exponential part called Urbach tail. This is very low for good crystalline materials having fewer impurities [35]. Closely near to band gap edge, the absorption coefficient is represented as,

$$\alpha = \alpha_0 \exp (hv/E_u) \tag{2}$$

where α_0 —constant, E_u - energy of Urbach or band tail.

Taking log on both sides of the above expression,

$$\ln \alpha = \ln \alpha_0 + (hv/E_u) \tag{3}$$

Figure 5(a, b) clearly illustrates the Urbach or band tail energy by taking the inverse of the slope from the straight linear line [36]. For LA and doped LA the

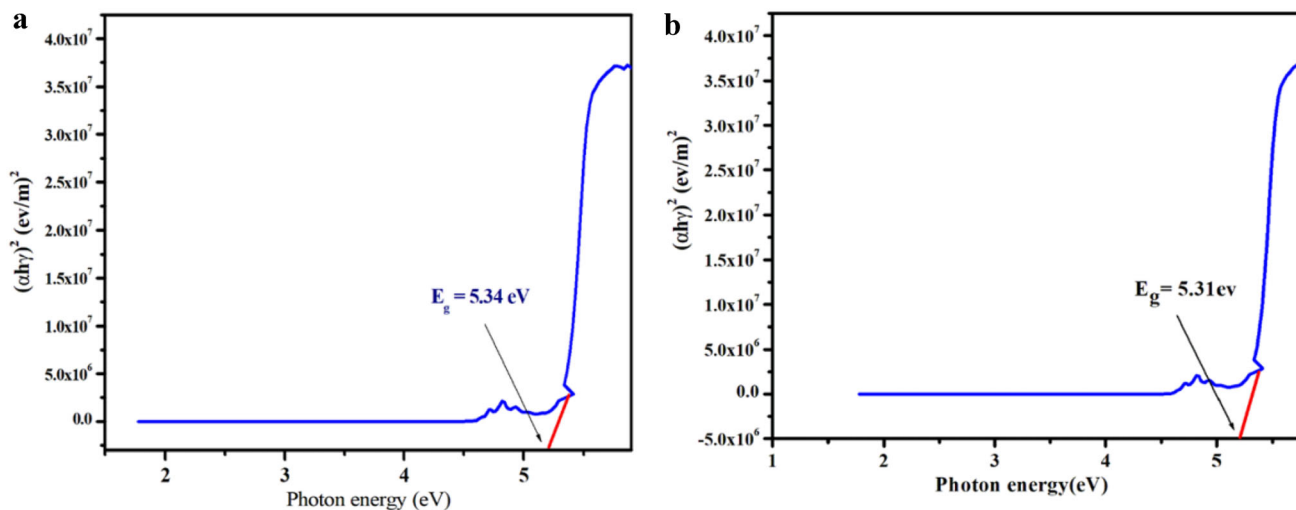


Fig. 4 (a,b). Tauc's Plot of LA and boric acid doped LA

Urbach (E_u) was identified to be 0.4163 eV and 0.5662 eV, respectively. Thus the lower magnitude confirms lesser structural defect with better purity and good crystalline nature [37].

3.4 Thermal studies

Thermal examination is an extremely essential procedure to ascertain thermal behaviour such as melting point, stability and decomposition point of the materials covering broad range of manufacturing and research fields. The thermal nature of pure L-alanine and boric acid doped L-alanine crystals were investigated by thermogravimetric analysis (TGA) and differential thermogravimetric analysis (DTA) by

taking samples of 3.0060 mg pure L-alanine and 3.7760 mg boric acid doped L-alanine employing a SPT Q600 V20.9 thermal analyser. The powder samples were placed in temperature range 20–600 °C at a heating rate of 20 °C/min. From the TGA and DTA traces (Fig. 6 a and b), weight loss is not observed up to 110 °C in BA doped LA, approves absence of entrapped water. After that, weight loss occurred in a single step for pure L-alanine (Fig. 6a) and weight loss takes place in two stages for BA doped LA crystal (Fig. 6b) and several gaseous fractions like CO, CO₂, NH₂ etc. are liberated leading to bulk decomposition before 600 °C. DTA plot (Fig. 6a) provides sharp endothermic peak at 280 °C (pure L-alanine), two sharp endothermic peaks at 112.42 °C

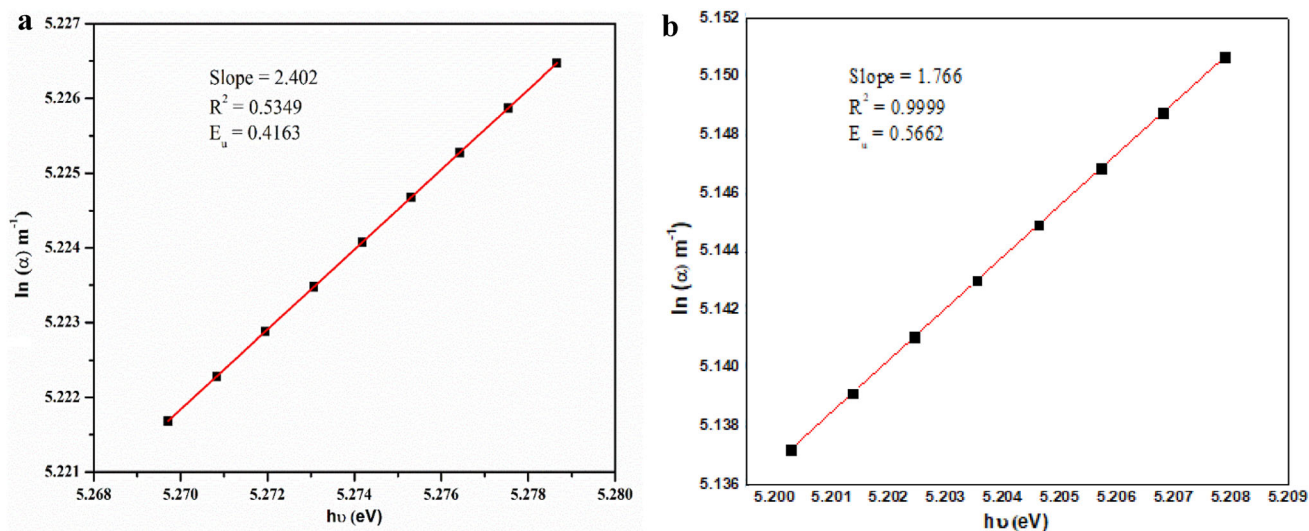


Fig. 5 (a,b). Plot $\ln(\alpha)$ with $h\nu$ for LA and boric acid doped LA

coincides with the first stage of decomposition in TGA trace and second endothermic peak 253 °C (boric acid doped L-alanine) (Fig. 6b)) corresponds to second stage of decomposition are due to volatilization of the materials and also may be due to the dehydration of boric acid above 150 °C (Fig. 6b)[38]. Hence we can conclude that pure LA and boric acid doped L-alanine crystals can withstand high temperature involving NLO applications up to 280 °C (pure L-alanine) and 253 °C (boric acid doped L-alanine) with good degree of crystallinity and purity of the crystals [21]. Also the thermal study shows that the BA doped LA crystal is thermally stable than certain metal based L-alanine crystals [39, 40].

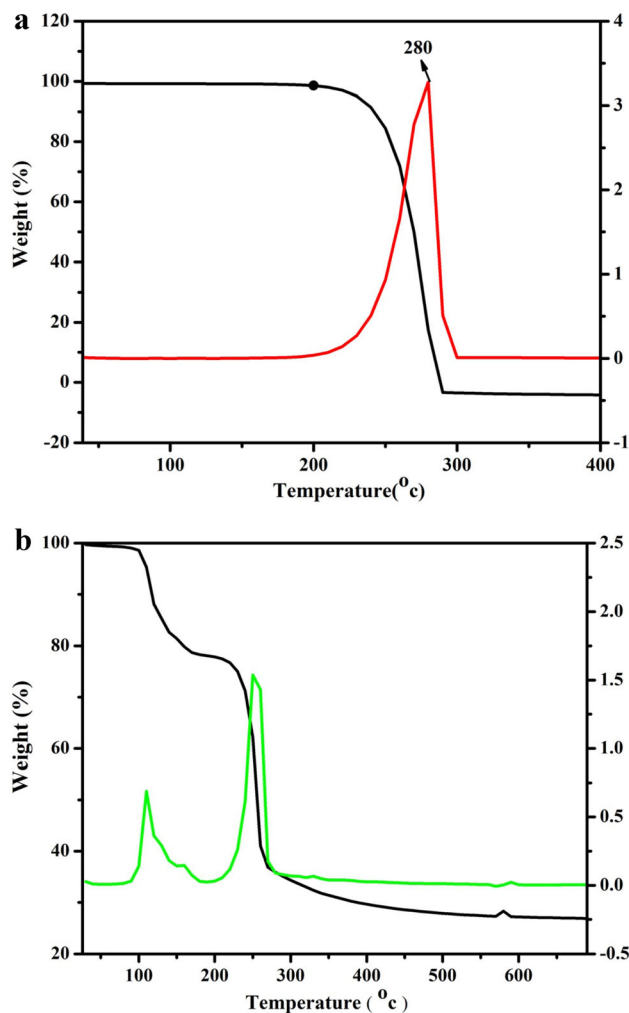


Fig. 6 a TG and DTA curves of pure L-alanine b TG and DTA curves of boric acid doped L-alanine

3.5 Microhardness analysis

Hardness of the material can be interpreted as its capability to resist long-lasting damage and also one of the foremost characteristic of any device materials [41]. Since mechanical strength is one of the important properties of any device fabrication is represented by its hardness [15].

The analysis of microhardness can be done to identify their mechanical characteristics by changing the loads (25 to 100 g). The diagonal length which is represented as *d* for indentation impression was analysed. Vickers hardness number (H_v) is determined by [42, 43]:

$$H_v = 1.8544 \frac{P}{d^2} \text{ (kg/mm}^2\text{)} \tag{4}$$

Here 1.8544 is a geometrical factor, *d* indicates the length (diagonal). Figure 7(a, b) and Fig. 8(a, b) notices that hardness (H_v) of the crystals drastically rises with increase of load (applied) confirms their high mechanical potency. The correlation between load (applied) and indentation range can be constituted by, $P = Kd^n$, *K* (constant) and *n* (Meyer’s index). According to Onitsch, $1 < n < 1.6$ holds good for hard category and $n > 1.6$ for soft category material [44]. The slope value declares the value of work hardening coefficient ($n = 3.14$ (LA), 3.26 (BA doped LA)) is a clear indication of their softness showing RISE behaviour [45].

The yield strength (σ_y) can be evaluated as,

$$\sigma_y = \frac{H_v}{3} (0.1)^{n'-2} \tag{5}$$

The elastic stiffness constant (C_{11}) is determined using Wooster’s empirical formula [45],

$$C_{11} = (H_v)^{7/4} \tag{6}$$

C_{11} predicts an assessment of bonding to the closest atoms. The calculated mechanical parameters are shown in Table 2 (LA) and Table 3 (doped LA).

3.6 Laser damage threshold (LDT)

Optically grown materials are examined by LDT, as it is a remarkable parameter to understand the material’s capability in linear and nonlinear characteristics to withstand high power intensities of laser involving nonlinear optical application such as electro optic modulation and second harmonic generation. The

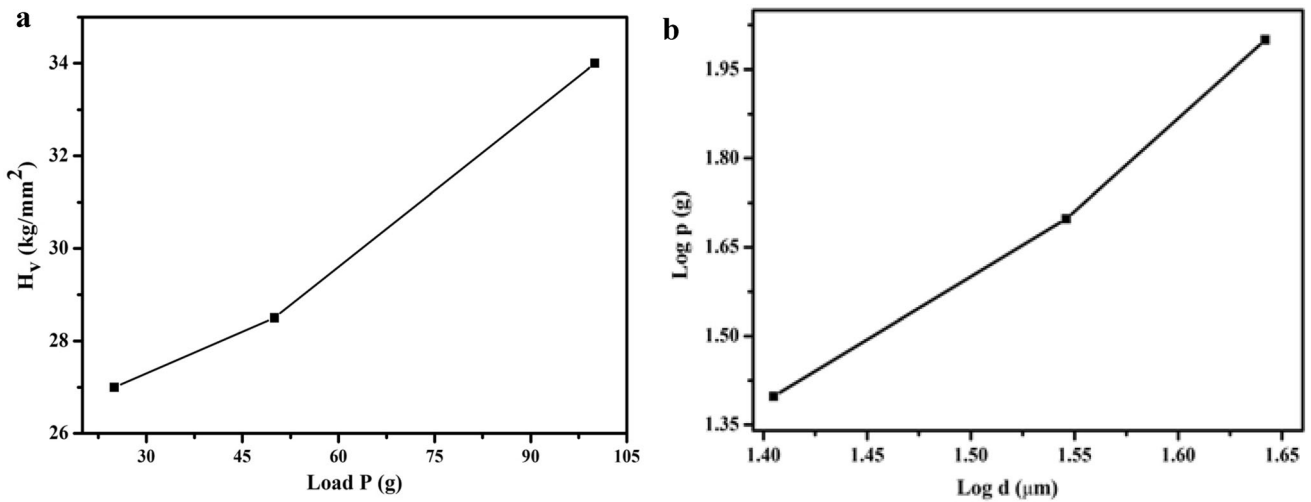


Fig. 7 a Microhardness b Meyers plot of LA

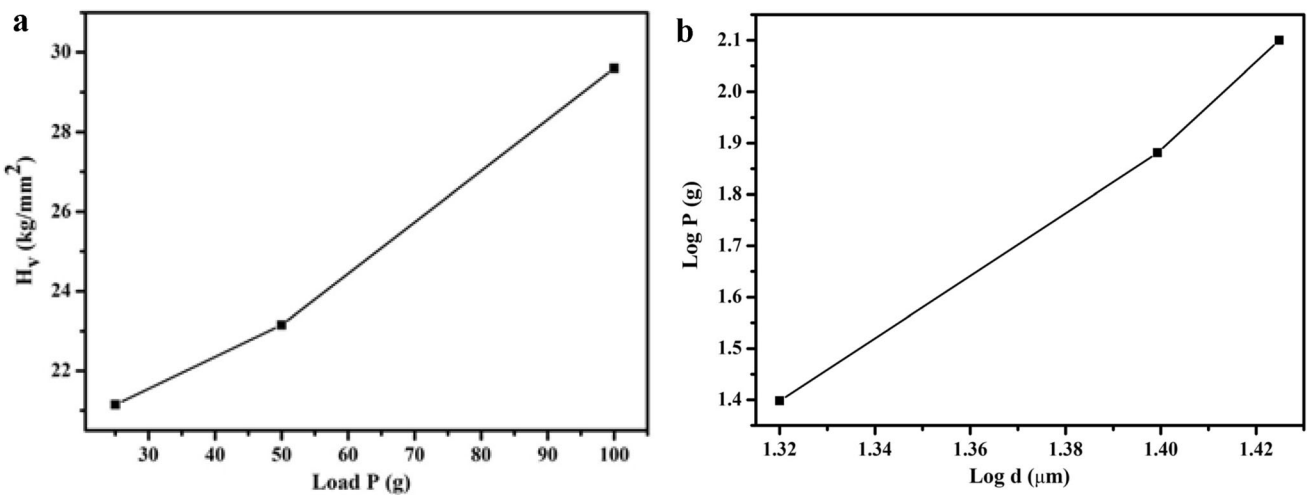


Fig. 8 a Microhardness b Meyers plot of Boric acid doped LA

Table 2 Mechanical parameters of pure LA

Load (gram)	Hardness number (Kg/mm ²)	Meyer's index <i>n</i>	Yield strength (GPa)	Stiffness constant (GPa)
25	27	3.14	6.389	3.134
50	28.5	3.14	6.744	3.445
100	34	3.14	8.045	4.691

pulse width of 6 ns with a repetition rate of 10 Hz and a fundamental wavelength of 1064 nm Gaussian beam (Quanta-Ray INDI, Spectra Physics) was employed to estimate the laser damage threshold. The damage threshold of laser was determined by the expression.

$$\text{Power density } P_d = E / A\tau \tag{7}$$

Here, E, A and τ denotes the energy, area (circular spot) and pulse width (ns). The computed LDT for the crystals (LA and boric acid doped LA) is found as 2.52 and 2.64 GW/cm² show higher damage

Table 3 Mechanical parameters of boric acid doped LA

Load (gram)	Hardness number (Kg/mm ²)	Meyer’s index <i>n</i>	Yield strength (GPa)	Stiffness constant (GPa)
25	21.15	3.26	3.796	2.044
50	23.15	3.26	4.155	2.394
100	29.6	3.26	5.313	3.681

threshold value than certain organic and semiorganic materials such as ASOX, BV, CDBA, 4MSTB, LATBF, LFMH, BTZA [46–52] and also compared to metal doped LA[21] and KDP(0.20 GW/cm²), Urea(1.50GW/cm²) [53, 54] is presented in Table 4 for comparison. The inclusion of dopants in the parent crystal reveal the laser withstanding limit from the enhanced LDT value could be made use of in the field of NLO applications involving optical switching devices [55]. Apart from thermal effect, multiphoton ionization is the important cause for laser-induced damage.

3.7 Dielectric analysis

The characteristics of dielectric nature of a crystal are a measure of electrical feature of the material promoted by the polarization configuration. The variance of dielectric parameters (dielectric constant (ϵ') and dielectric loss (ϵ'')) with respect to frequency is displayed in Fig. 9a, b and Fig. 10 a, b. Because of space charge polarization, the dielectric constant possesses higher value at the region of low frequency.

Table 4 Comparison of LDT of grown crystal with other reported NLO Crystals

Crystal Name	LDT (GW/cm ²)	Reference
ASOX	2–04	[46]
BV	0.38	[47]
CDBA	0.6	[48]
4MSTB	1.11	[49]
LATBF	0.79	[50]
LFMH	1.5	[51]
BTZA	0.01244	[52]
KDP	0.20	[53]
UREA	1.50	[54]
Metal doped LA	0.03943	[21]
LA	2.52	Present work
BA doped LA	2.64	Present work

Bold refers to highlight our present materials (LA and BA doped LA)

In the range of high frequencies, the value of dielectric loss is very low as the frequency of the electrical field applied does not get harmonized with the natural frequency. As the crystals show low measure of ϵ' , ϵ'' they could be utilized in electro optic modulations.

3.7.1 Activation energy

The graph drawn between $\log \sigma_{ac}$ and inverse of temperature is represented in Fig. 11(a,b) using the relation $\sigma_{ac} = \sigma_o \exp(-E_a/k_B T)$, where, σ_{ac} is the conduction at temperature T, E_a is the activation energy for the electrical process and k_B is the Boltzmann constant (1.38×10^{-23} J/k). The profile shows almost a linear behaviour and the slope from this graph is used to evaluate the activation energy using the formula [25],

$$E_a = -\text{Slope} \times 1000 \times k_B \tag{8}$$

The values obtained are 0.01019 eV, 0.01284 eV, 0.01345 eV and 0.03059 eV at frequencies 800 Hz, 4000 Hz, 30 kHz and 2 MHz for pure LA and 0.01142 eV, 0.01309 eV, 0.01357 eV, 0.01199 eV at 500 Hz, 000 Hz, 20 kHz and 1 MHz frequencies for BA doped LA respectively, proves that the changes caused in the crystals need greater activation energy to jump between the energy states. Hence crystals possess less number of defects owing to less activation energy suitable for device fabrications [25].

3.7.2 Jonscher’s power law of conduction mechanism

Frequency is closely connected with conductivity in a material which could be examined from Jonscher’s power law [56] who had studied the variation of electrical conductivity σ_{ac} with frequency for different solids comprising of polymers, glasses and crystals [57], is plotted in Fig. 12 a, b for pure LA and BA doped LA crystals where conduction mechanism is understood. From Jonscher’s power law,

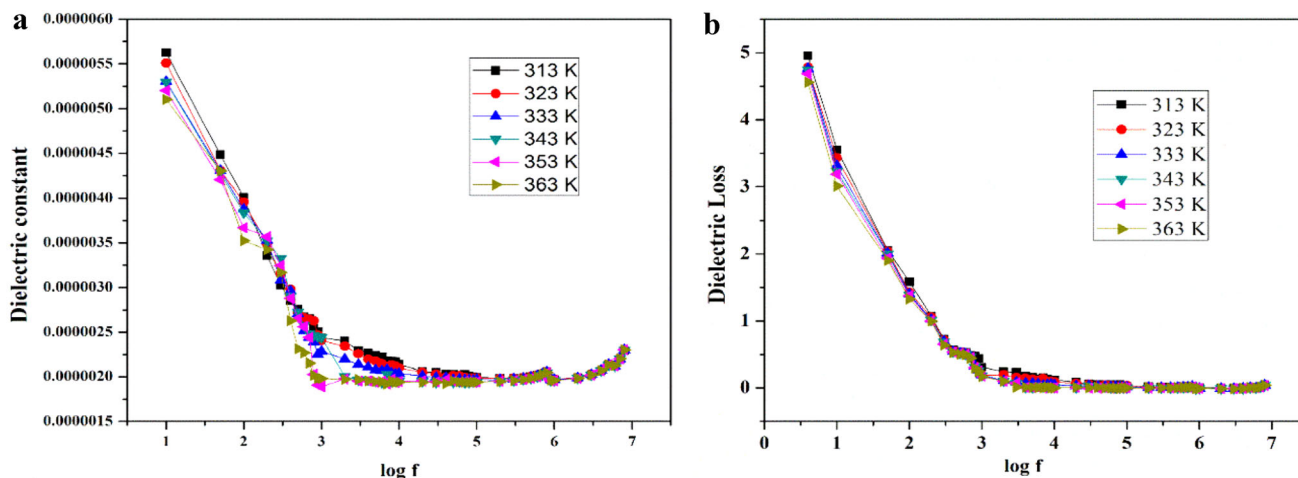


Fig. 9 a, b Dielectric constant, Dielectric loss of LA

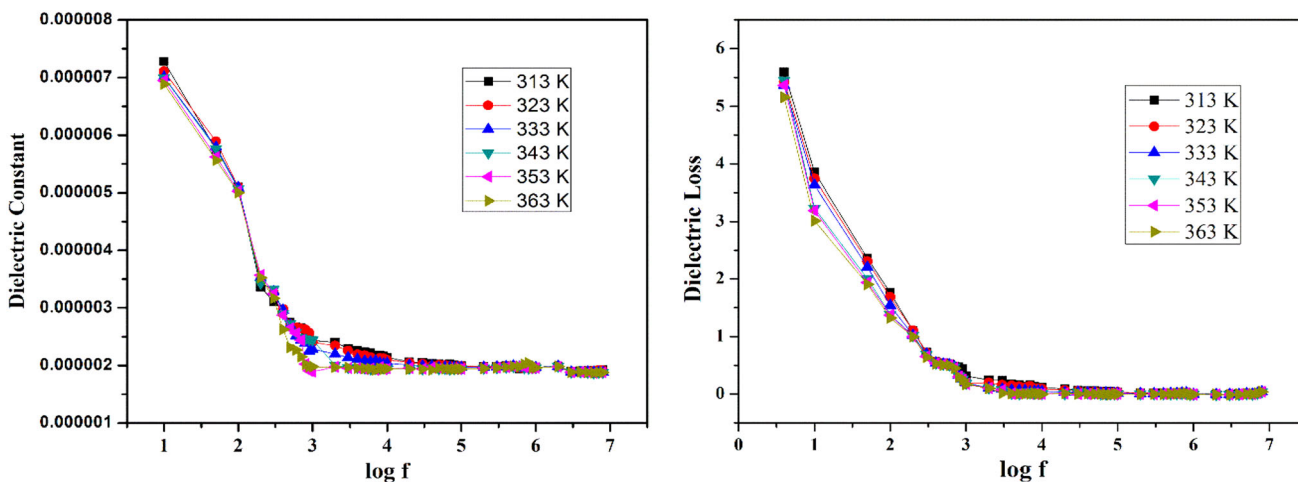


Fig. 10 a, b Dielectric constant, Dielectric loss of BA doped LA

$$\sigma_{a.c} = \sigma_{d.c} + A\omega^s \tag{9}$$

where σ_{dc} is the DC conductivity which predicts the frequency (ω) independent plateau in the low frequency region, A is temperature dependent constant rely on the strength of polarisation, and s is temperature dependent power law exponent lies in the range $0 < s < 1$, varies material to material. The estimated values of $s = 0.988$ (pure LA) and $s = 0.985$ (BA doped LA) from the slope of the graph confirms that grown crystals obeys power law. From the plotted figures (Fig. 12 a, b), it is noted that AC conductivity increases comparatively at higher frequency due to hopping mechanism [58] observed for pure and doped LA crystals.

3.8 SEM and EDAX analysis

To examine the surface morphology of boric acid doped LA crystal, FE1 quanta high resolution SEM has been used. The pictures of SEM in the resolution range of 5 and 10 μm are shown in Fig. 13. The elements present in the grown crystal are represented with diverse colours (Fig. 14) which confirms the presence of boron in the material. The overlapping of the crystals at different magnifications occur due to the agglomeration affected by the temperature fluctuations during the growth process. Scanning electron microscope affirmed that the surface of the crystal is having smooth topographical nature.

Energy dispersive X-ray Analysis (EDAX) was done to confirm the elements in the grown crystal of boric acid doped LA at diverse energies. The

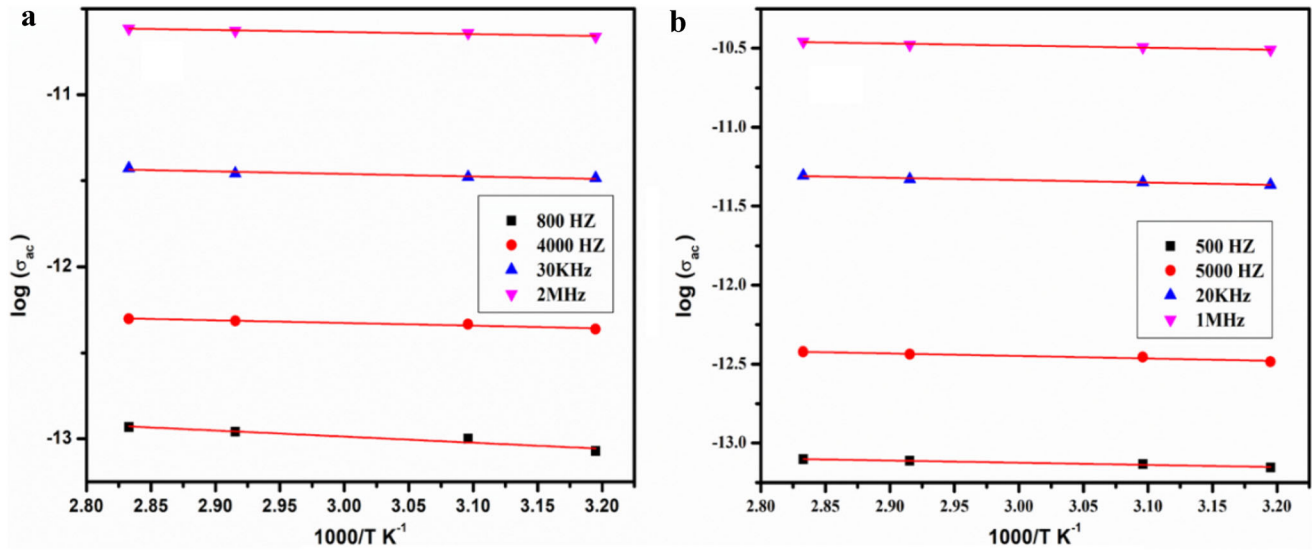


Fig. 11 a, b Plot of σ_{ac} vs $1000/T$ for pure LA and BA doped LA

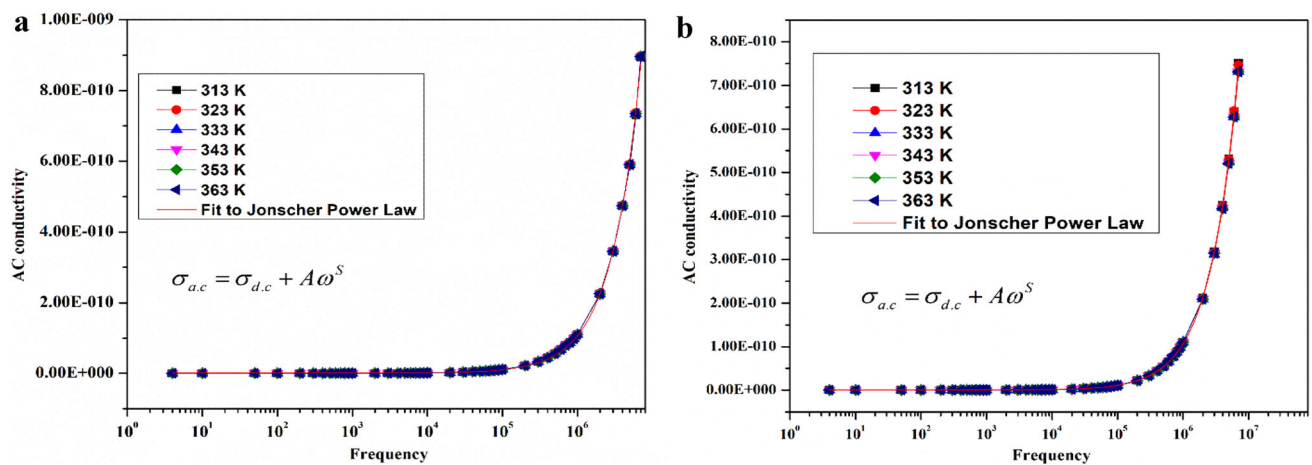


Fig. 12 a, b Plot of AC conductivity versus Frequency of pure LA and doped LA

presence of boron is observed from the EDAX spectra (Fig. 15).

3.9 Fluorescence studies

The emission spectrum of both the grown materials (pure and boric acid doped LA) is revealed in fluorescence spectrum (Fig. 16 a, b) by applying the excitation wavelength of 245 nm (LA) and 238 nm (BA doped LA). Crystals show a stronger photon energy absorption band in the UV region with a highest intensity violet emission radiation at 404 nm (pure LA) and at 392 nm (doped LA) is likely to be useful in optoelectronic device applications. The title materials exhibit a strong and broad emission peak 404 nm (LA) and 392 nm (doped LA) which is related

to the $p-p^*$ localized electron between the donor and acceptor groups through organic chromophore (p -conjugated double bond), which lead to its luminescence characteristic nature [59]. The peak of emission having highest intensity at 404 nm (LA) and 392 nm (doped LA) falls in the visible region that corresponds to violet fluorescence spectra. The peak observed at 296 nm (LA) and 297 nm (boric acid doped LA) are assigned to the defects present inside the materials serves as a predominant parameter of optoelectronics device applications and tunable laser system [60].

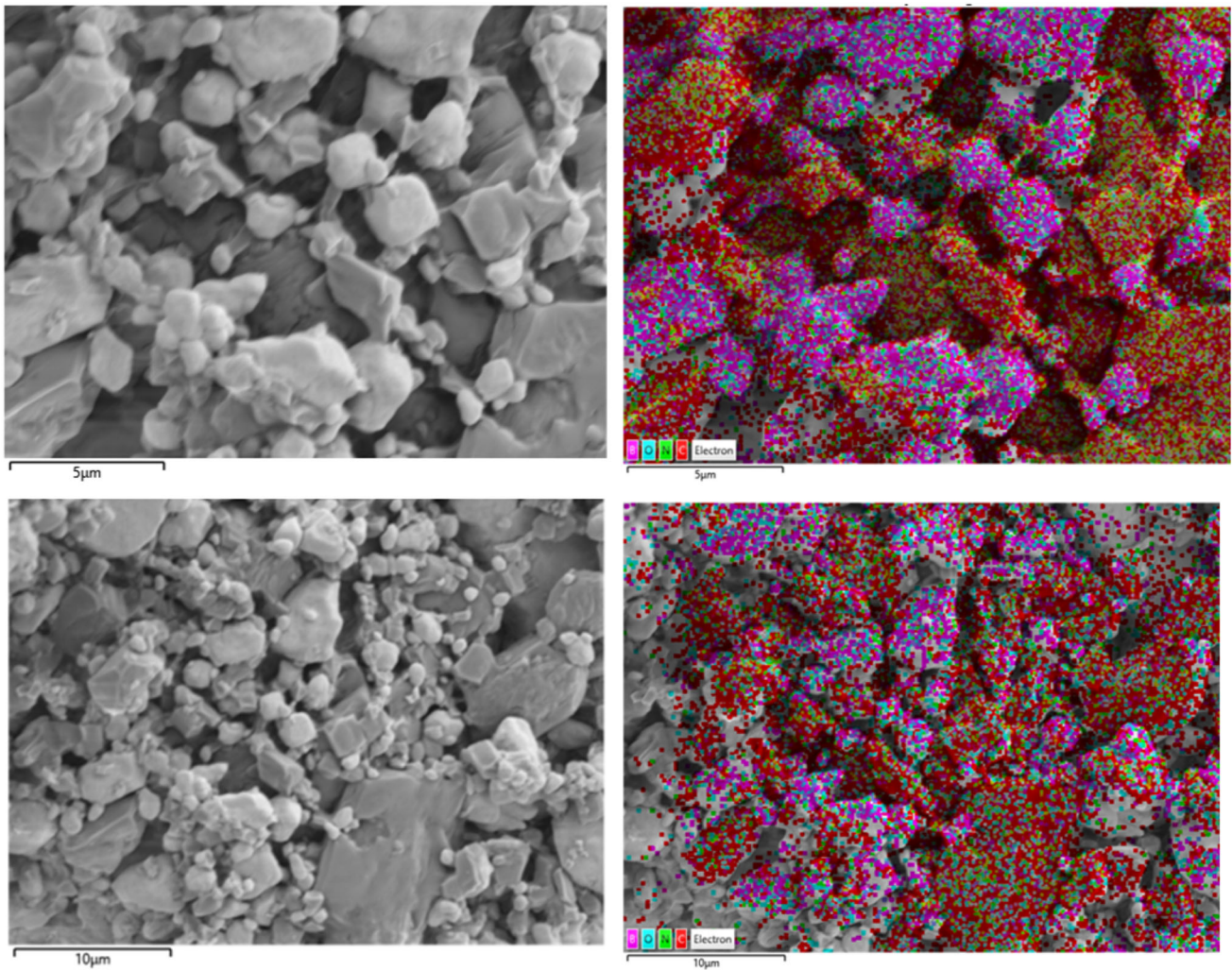


Fig. 13 SEM micrograph of boric acid doped LA for resolution 5 μm and 10 μm

4 Nonlinear Optical Studies

4.1 Second harmonic generation- SHG

Crystals of organic category acquires SHG efficiency because of their large band gap and lesser value of dielectric constant which plays a key role in photonic applications [61]. Kurtz Perry powder technique [62] was employed to figure out the frequency doubling mechanism utilizing Nd-YAG laser with pulse duration (6 ns) and pulse rate (10 Hz). The frequency doubling effect was found to be 0.33 (LA) and 0.38 (boric acid doped LA) times of KDP and found to be comparable. The second harmonic in LA and boric acid doped LA was confirmed by the green radiation emitted from the samples. This firmly approved that the grown materials are capable aspirants for NLO

applications which includes very useful for opto-electronic and terahertz applications.

4.1.1 Third harmonic generation -THG

By the approach of Z-scan technique, frequency tripling feature of harvested materials have been studied utilising 532 nm diode pumped continuous wave Nd-YAG laser was used as source produces both the sign and magnitude of the phase change. Normalised transmittance in closed aperture, open aperture, ratio of closed to open aperture and transmittance versus input intensity are shown in Fig. 17 a–d and Fig. 18a–d for LA and boric acid doped LA. From the open aperture profile, the nonlinear absorption coefficient (β) is assessed for both samples [63]. The closed aperture determines nonlinear refraction. The

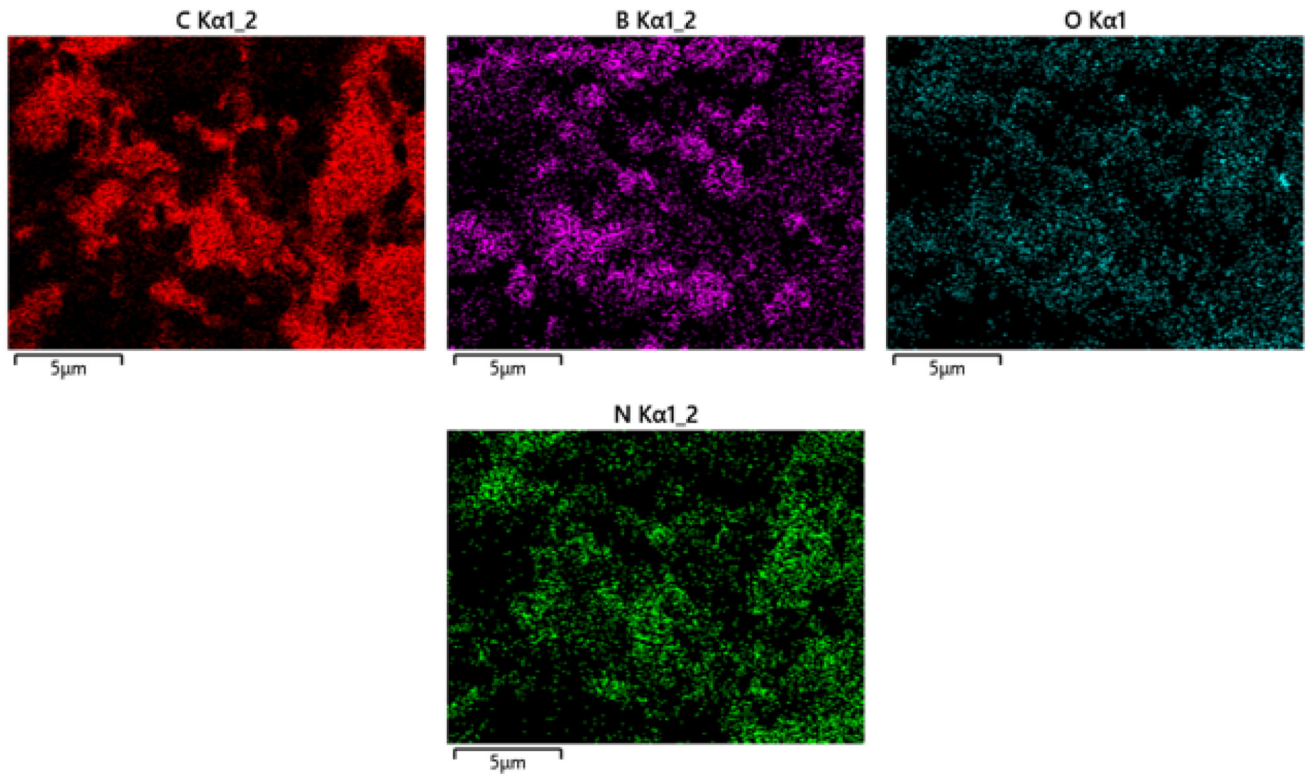
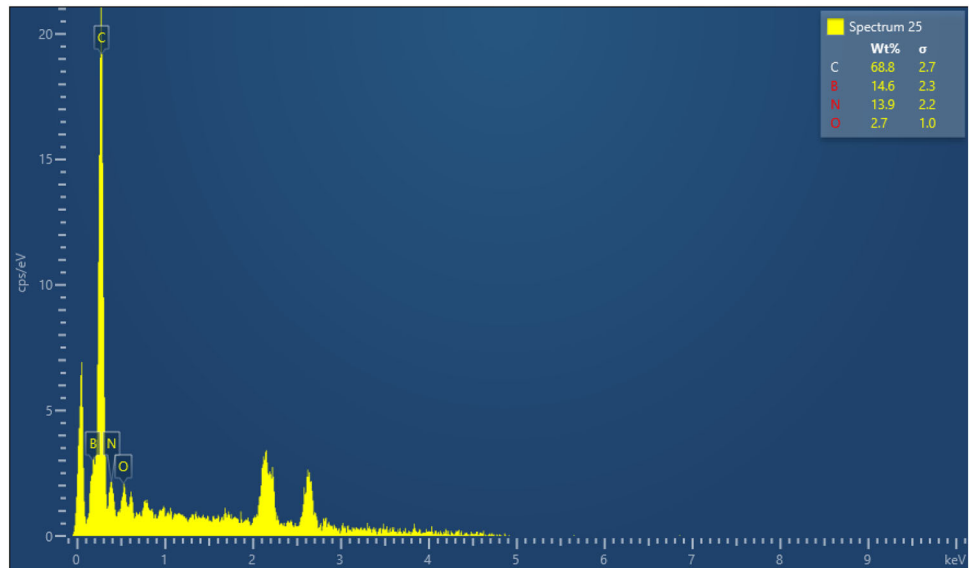


Fig. 14 SEM micrograph for resolution 5 μm showing different elements in Boric acid doped LA crystal

Fig. 15 EDAX spectra of Boric acid doped LA



difference in the transmittance change of peak and valley (ΔT_{P-V}) is given by,

$$\Delta T_{P-V} = 0.406(1 - S)^{0.25} |\Delta\Phi_0| \tag{10}$$

Linear transmittance aperture(S) is assessed by,

$$S = 1 - \exp\left(\frac{-2r_a^2}{\omega_a^2}\right) \tag{11}$$

The nonlinear refractive index (n_2) can be assessed from the formula

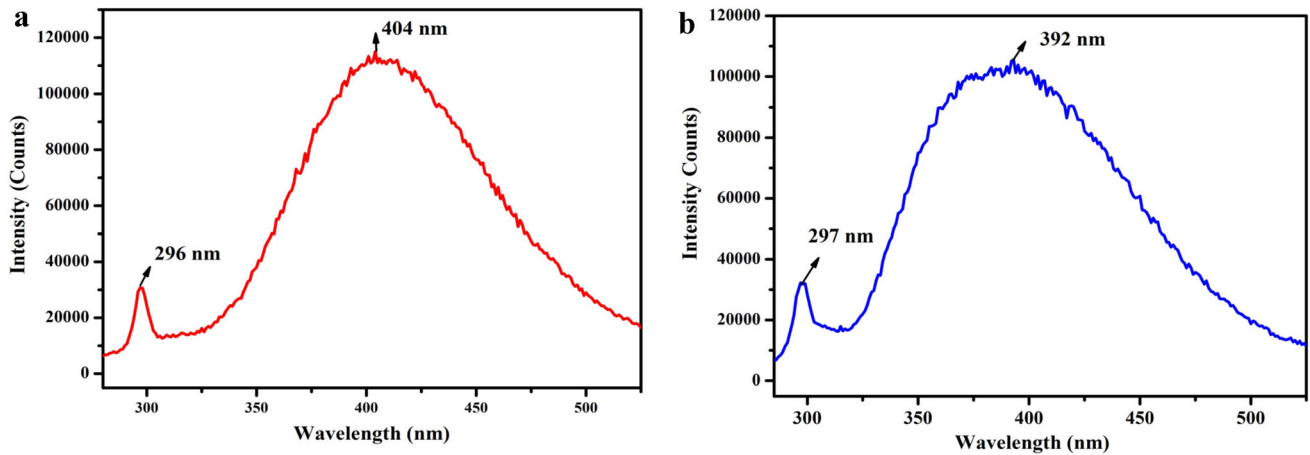


Fig. 16 a, b Emission spectrum of the LA and boric acid doped LA crystals

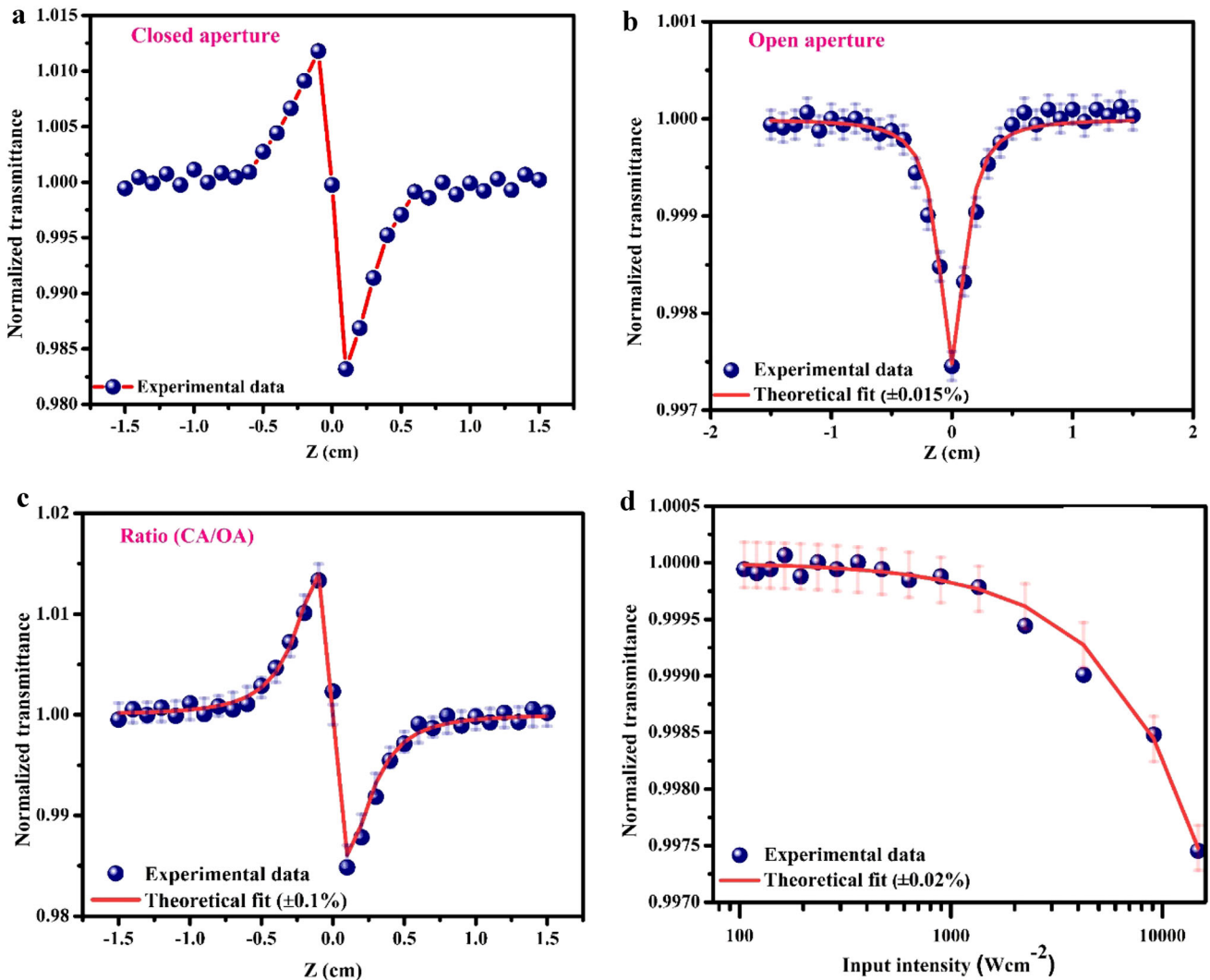


Fig. 17 a Closed aperture spectrum b Open aperture spectrum c ratio of the closed to open Z scan traces (d) Normalised transmittance versus Input intensity of LA

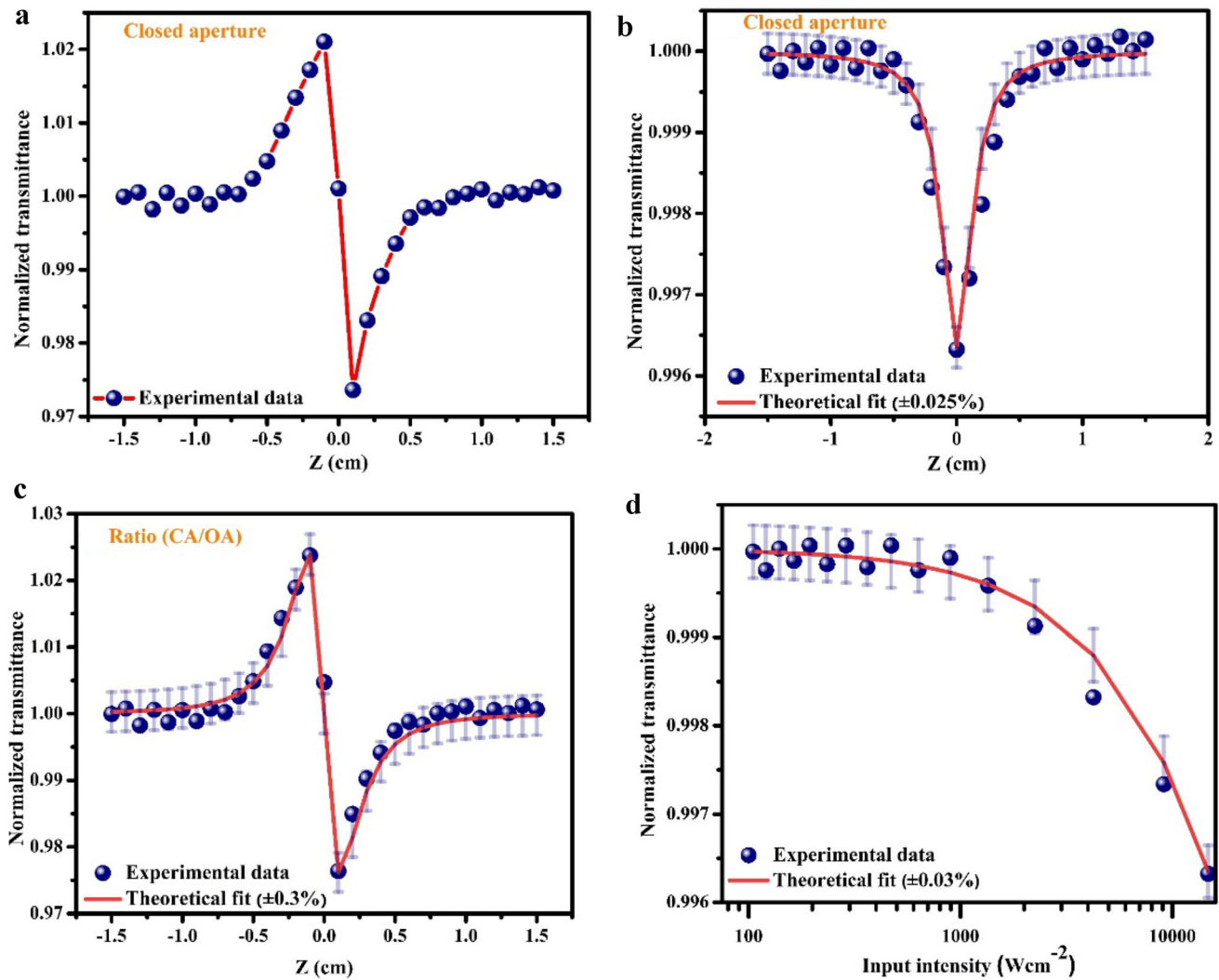


Fig. 18 a Closed aperture spectrum b Open aperture spectrum c ratio of the closed to open Z scan traces d Normalised transmittance versus Input intensity of Boric acid doped LA

$$n_2 = \frac{\Delta\Phi_0}{KI_0L_{eff}} \tag{12}$$

Nonlinear absorption coefficient can be found by,

$$\beta = \frac{2\sqrt{2}\Delta T}{I_0L_{eff}} \tag{13}$$

In the data of closed aperture, peak followed by valley is observed in both the samples, which indicates negative nonlinearity (self-defocussing). This defocussing feature of samples is owing to the (negative) refractive index which is utilized in night vision applications [59, 64–66]. From negative refractive index value, it could be seen that materials exhibits defocusing nature, which is an essential

parameter for optical sensor applications [66]. This defocusing nature due to negative refractive index also suggests that the title crystal could exhibit higher laser damage threshold [66]. Night Vision Equipment utilizes the optoelectronic devices where active infrared night-vision combines infrared illumination of spectral range 700–1,000 nm [64, 65].

The third-order nonlinear optical susceptibility was given by

$$\text{Re}\chi^{(3)}(esu) = \frac{10^{-4}(\epsilon_0 C^2 n_o^2 n_2)}{\pi} \left(\frac{cm^2}{W}\right) \tag{14}$$

$$\text{Im}\chi^{(3)}(esu) = \frac{10^{-2}(\epsilon_0 C^2 n_o \lambda \beta)}{4\pi^2} \left(\frac{cm^2}{W}\right) \tag{15}$$

Table 5 Z-scan measurements of LA and boric acid doped LA

Third-order nonlinear properties	Measured values(LA)	Measured values (boric acid mixed LA)
Nonlinear refractive index (n_2)	1.060×10^{-9} (cm ² /W)	6.378×10^{-10} (cm ² /W)
Nonlinear absorption coefficient (β)	0.0389×10^{-4} (cm/W)	0.0276 (cm/W)
Real susceptibility (χ^3)	4.894×10^{-8} (cm ² /W)	2.974×10^{-8} (cm ² /W)
Imaginary susceptibility (χ^3)	7.656×10^{-8} (cm/W)	5.447×10^{-8} (cm/W)
Absolute susceptibility (χ^3)	9.087×10^{-8} (esu)	6.207×10^{-8} (esu)

Table 6 Comparison of χ^3 value of present pure and boric acid doped LA with other NLO materials

Materials in literature	Third-order nonlinear susceptibility (χ^3)
(C9H7NO)4H7PMo12O40·3H2O (I)	9.6×10^{-11} (esu)
(phen)3H7PMo12O40·CH3CN·H2O (II) [66]	1.48×10^{-12} (esu)
2A6MP4HB [68]	8.3551×10^{-10} (esu)
3, 4-dimethoxy-substituted chalcone [69]	3.1×10^{-12} (esu)
VMST [70]	9.69×10^{-12} (esu)
2APM [71]	5.741×10^{-8} (esu)
GUCN [72]	2.05×10^{-8} (esu)
KDP [73]	4.02×10^{-14} (esu)
LA[Present]	9.087×10^{-8} (esu)
Boric acid mixed LA[Present]	6.207×10^{-8} (esu)

Bold refers to highlight our present materials (LA and BA doped LA)

$$|\chi^{(3)}| = \sqrt{(\text{Re}(\chi^{(3)}))^2 + (\text{Im}(\chi^{(3)}))^2} \quad (16)$$

Table 5 provides the experimental outcomes of Z-scan for LA and boric acid doped LA. The nonlinear absorption coefficient (β) is 0.0389×10^{-4} (cm/W) and 0.0276×10^{-4} (cm/W) indicates two photon absorption. The intensity of the transmitted light is linearly increased at low input power and then it saturates beyond the 3.419×10^3 W/cm² for pure L-alanine and 2.906×10^3 W/cm². This result indicates the existence of noticeable optical limiting characteristics of the crystals. In general, the origin of the optical limiting is a complex process, however, it may be correlated with important factors such as nonlinear optical refraction (or thermal effect), nonlinear optical absorption and nonlinear optical scattering [65]. Hence, the obtained result satisfies the essential requirement of optical limiters create them as versatile candidates in optical limiting process [67]. Also third-order nonlinearity ($\chi(3)$) with other similar class of crystals reported earlier are compared and presented in Table 5.

($\chi(3)$) values of grown materials are found to be higher than NLO materials reported [66, 68–72] also

furnished for comparison with present pure LA and BA doped LA materials presented in Table 6.

5 Conclusion

Single crystals of pure L-alanine and 5 wt % of boric acid doped L-alanine have been grown using slow evaporation technique with water as solvent and their structures analysed by single crystal XRD revealed noncentrosymmetric space group. The FT-IR frequencies observed confirms the zwitterion formation in the crystals and presence of doped element from the wavenumbers seen at lower frequencies. The UV–VIS study shows insignificant absorption in the visible region enabling the crystals implementation in opto-electronic field. The thermal studies discloses the materials stability up to 280 °C (LA) and 253 °C (BA doped LA). The fluorescence emission peak of violet is observed at 404 nm for LA and 392 nm for doped LA. The dielectric investigation indicates lower value of dielectric constant and dielectric loss in the grown materials suggests the materials advantage in microelectronics device applications. Also Jonscher's power law;

$\sigma_{a.c} = \sigma_{d.c} + A\omega^s$, investigates that event of conduction predominantly increased at high frequency with temperature dependent exponent $s < 1$. Laser damage tolerance which is an imperative factor shows the crystals potential in withstanding high power lasers. SEM examination determines the surface topography at different magnifications and EDAX spectrum reveals the presence of element Boron in doped LA crystal. The analysis of microhardness infers that both crystals correspond to soft category. The third order nonlinear characteristics of the crystals suggest good focusing nature with nonlinear refractive index and nonlinear absorption coefficient and third-order susceptibility for pure LA and BA doped LA ($\chi^3 = 9.087 \times 10^{-8}$ (esu), 6.207×10^{-8} (esu) suggest them in third-order nonlinear optical device applications. From the analyses carried out, L-alanine and boric acid doped L-alanine single crystals are proving to be promising contenders in frequency conversion process for optoelectronic applications together with optical switching, optical limiting and device fabrications.

Acknowledgements

M. Lydia Caroline, Assistant Professor, Department of Physics, Dr. Ambedkar Govt Arts College, Vyasarpadi, Chennai thanks TANSCHÉ for extending financial support for this work through a grant to MINOR RESEARCH PROJECT RC. No. 1740/2021 A. Authors also thank SAIF, IITM, Chennai and Department of Physics, St. Joseph College for the support in taking characterizations is gratefully acknowledged.

Author contributions

All authors contributed to the study conception and design, Material preparation, data collection and analysis were performed by M.L.C, A.D.R, C.R.T.K, M.N, P.S, G.V, S.K. The first draft of the manuscript was written by M.L.C, A.D.R and all authors commented on the previous versions of the manuscript. All authors read and approved the final manuscript.

Funding

This work was supported by TANSCHÉ in extending financial support for this work through a grant to MINOR RESEARCH PROJECT RC. No. 1740/2021 A. M. Lydia Caroline, Assistant Professor, Department of Physics, Dr. Ambedkar Govt Arts College, Vyasarpadi, Chennai has received research support from TANSCHÉ MINOR RESEARCH PROJECT.

Data availability

The datasets generated during and/or analysed during the current study are available from the corresponding author on reasonable request.

Declarations

Conflict of interest M. Lydia Caroline, Assistant Professor, Department of Physics, Dr. Ambedkar Govt Arts College, Vyasarpadi, Chennai has received financial support for this work from TANSCHÉ through a grant to MINOR RESEARCH PROJECT RC. No. 1740/2021 A.

References

1. H.S. Nalwa, Organometallic materials for nonlinear optics. *Appl. Organomet. chem.* **5**, 349–377 (1991)
2. P.-J. Kim, J.-H. Jeong, M. Jazbinsek, M. Jazbinsek, O-Pil Kwon Acentric nonlinear optical N-benzyl stilbazolium crystals with high environmental stability and enhanced molecular nonlinearity in solid state. *Cryst. Eng. Comm.* **13**(2), 444–451 (2010). <https://doi.org/10.1039/C0CE00456A>
3. J.R. Davy, S.R. Rees, J. Staromlynska, J.A. Hermann, M.P. Gillyon, T.J. McKay, P.B. Chapple, Optical Devices Utilizing Nonlinear Organic Materials, Polymers and Other Advanced Materials: Emerging Technologies and Business Opportunities, in *Fai.* ed. by P.N. Prasad, J.E. Mark, T. Joo (Plenum Press, New York, 1995)
4. C. Indumathi, T.C. Sabari Girisun, K. Anitha, S. Alfred Cecil Raj, Structural, thermal, optical and nonlinear optical properties of ethylenediaminium picrate single crystals. *J. Phys. Chem. Sol.* (2017). <https://doi.org/10.1016/j.jpics.2017.03.003>
5. P.M.C.S.P.M.G.G.A. SangeethaNageshwariKumariSudhaJayaprakashLydia CarolineMathubalaVinithaManikandan, Linear and nonlinear optical investigation of l-arginium adipate single crystal for

- photonic applications. *J. Mater. Sci.: Mater. Electron.* **31**, 14545–14552 (2020)
6. P. Jayaprakash, M. Lydia Caroline, S. Sudha, R. Ravisankar, G. Vinitha, P. Ramesh, E. Raju, 'Synthesis, growth, optical and third order nonlinear optical properties of l-Phenylalanine d-Mandelic acid single crystal for photonic device applications. *J. Mater. Sci.: Mater. Electron.* **31**, 20460–20471 (2020)
 7. R. Jothi Mani, H. Palanisamy Selvarajan, Alex Devadoss, Dr. Shanthi, Second-order, third-order NLO and other properties of L-alanine crystals admixed with perchloric acid (LAPA). *Optik* **126**(2), 213–218 (2015). <https://doi.org/10.1016/j.ijleo.2014.08.143>
 8. M. Lydia Caroline, R. Sankar, R.M. Indirani, S. Vasudevan, Growth., optical, thermal and dielectric studies of an amino acid organic nonlinear optical material: l-Alanine. *Mater. Chem. Phys.* **114**, 490–494 (2009)
 9. V. Krishnakumar, L. Guru Prasad, R. Nagalakshmi, Investigation on 3-Aminophenol: A Nonlinear Optical Crystal for Frequency Doubling. *Eur. Phys. J. Appl. Phys.* **48**, 20403–20409 (2009). <https://doi.org/10.1051/epjap/2009159>
 10. M. Nageshwari, C. Rathika Thaya Kumari, G. Vinitha, S. Muthu, M. Lydia Caroline, Growth charact. of l-Serine: a promising acentric org. cryst. **541**, 32–42 (2018)
 11. B. Luther-Davies, M. Samoc, Third-order nonlinear optical organic materials for photonic switching. *Curr. Opin. Solid State Mater. Sci.* **2**(2), 213–219 (1997)
 12. P. Jayaprakash, P. Sangeetha, C. Rathika Thaya Kumari, I. Baskaran, M. Lydia Caroline, Growth and characterization of l-asparagine monohydrate admixed dl-mandelic acid nonlinear optical single crystal. *J. Mater. Sci.: Mater. Electron.* (2017). <https://doi.org/10.1007/s10854-017-7828-z>
 13. C.R.T. Kumari, M. Nageshwari, R. Ganapathi Raman, M. Lydia Caroline, Crystal growth, spectroscopic, DFT computational and third harmonic generation studies of nicotinic acid. *J. Mol. Struct.* **1163**, 137–146 (2018)
 14. N.S. Kim, D.J. Bray, *Org. Magn. Reson.* **15**(370), 374 (1981)
 15. R. Hanumantharao, S. Kalainathan, Microhardness studies on nonlinear optical L-alanine single crystals. *Bull. Mater. Sci.* **36**(3), 471–474 (2013)
 16. J.D. Bernal, *Z. Kristallogr.* **78**, 363 (1931)
 17. H.J. Simpson Jr., R.E. Marsh, The crystal structure of L-alanine. *Acta Cryst.* **20**, 550 (1966). <https://doi.org/10.1107/S0365110X66001221>
 18. R. Destro, R.E. Marsh, R. Bianchi, *J. Phys. Chem.* **92**, 966 (1988)
 19. M. Prabhakaran, C. Karman, S. Manivannan, S. Azhagiri, Crystal growth, optical, thermal, mechanical and laser damage threshold properties of nonlinear optical l-methionine inserted potassium pentaborate (LMKB5) single crystal for optoelectronic applications'. *J. Electron. Mater.* (2021). <http://doi.org/10.1007/s11664-021-08972-y>
 20. Matous Kloda, Irena Matulkova, Ivana Cisarova, Petra Becker, Ladislav Bohaty, Petr Nemeč, Robert Gyepes, Ivan Nemeč, Cocrystals of 2-Aminopyrimidine with Boric Acid—Crystal Engineering of a Novel Nonlinear Optically (NLO) Active Crystal". *Crystals* (2019). <https://doi.org/10.3390/cryst9080403>
 21. M. Lydia Caroline, G. Mani, S. Usha, Effect of Co²⁺ on the growth, optical properties and laser damage threshold of potential nonlinear optical l-alanine single crystal. *Optik* **125**, 5069–5074 (2016)
 22. C. Rathika Thaya Kumari, M. Nageshwari, S. Sudha, M. Lydia Caroline, G. Mani, Influence of uranyl on the growth, linear, laser damage threshold and nonlinear optical studies on potential nonlinear optical single crystal: L-Alanine. *J. Chem. Pharm. Sci.* 166–170 (2016)
 23. W.H. Zachariasen, The crystal lattice of boric acid, BO₃H₃. *Z. Kristallogr. - Cryst. Mater.* **88**(1–6), 150–161 (1934). <https://doi.org/10.1524/zkri.1934.88.1.150>
 24. D.E. Bethell, N. Sheppard, The infra-red spectrum and structure of boric acid. *J. Trans. of the Faraday Soc.* **55**, 1955 (1971)
 25. S. Sudha, C.R.T. Kumari, M. Nageshwari, P. Ramesh, G. Vinitha, Jaya prakash, M. Lydia Caroline, Synthesis, growth and third order nonlinear optical studies of a rhombohedral crystal: Sodium tetraborate pentahydrate. *Chinese J. Phys.* **57**, 211–225 (2019)
 26. Tuba ÖZDEMİR Ali Ünsal KESKİNER, Spectroscopic analysis of the boric acid and salicylic acid-boric acid-ethanol solution. *J. Boron* **3**(2), 118–125 (2018)
 27. G.F. OlingaMbala, M.T. Ottou Abe, Z. Ntieche, G.W. Ejuh, J.M.B. Ndjaka, Ab initio investigation of nonlinear optical, electronic, and thermodynamic properties of BEDT-TTF molecule: doping with boron. *Heliyon* **7**(7), e07461 (2021). <https://doi.org/10.1016/j.heliyon.2021.e07461>
 28. N.P.S. Chauhan, N.S. Hosmane, M. Mozafari, Boron-based polymers: opportunities and challenges. *Mater. Today Chem.* **14**, 100184 (2019). <https://doi.org/10.1016/j.mtchem.2019.08.003>
 29. R. Shanmugavadivu, G. Ravi, A.N. Azariah, A.H. Hameed, T. Thenappan, Synthesis, growth and characterization of new mixed analogs of LAP family crystals. *Mater. Sci. Eng.: B* **113**(3), 269–273 (2004)
 30. C.C. Jiménez, N. Farfán, M. Romero-Avila, M. Rodríguez, L. Aparicio-Ixta, G. Ramos-Ortiz, J.L. Maldonado, R. Santillan, N.E. Magaña-Vergara, M.E. Ochoa, Synthesis and chemical–optical characterization of novel two-photon fluorescent borinates derived from Schiff bases. *J. Organomet. Chem.*

- 755, 33–40 (2014). <https://doi.org/10.1016/j.jorganchem.2013.12.036>
31. S.D. Ross, *Inorganic infrared and raman spectra* (McGraw Hill Book Company (UK) Ltd., London, 1972)
 32. M. Prakash, D. Geetha, M. Lydia Caroline, Crystal growth, structural, optical, spectral and thermal studies of tris (L-phenylalanine) L-phenylalaninium nitrate: a new organic nonlinear optical material. *Spectrochim. Acta Part A* **81**, 48–52 (2011)
 33. M. Prakash, D. Geetha, M. Lydia Caroline, Synthesis, structural, optical, thermal and dielectric studies on new organic nonlinear optical crystal by solution growth technique. *Spectrochim. Acta Part A: Mol. Biomol. Spectrosc.* **107**, 16–23 (2013)
 34. M. Divya Bharathi, G. Ahila, J. Mohana, G. Chakkaravarthi, G. Anbalagan, Synthesis, crystal structure, growth, optical and third order nonlinear optical studies of 8HQ2C5N single crystal - an efficient third-order nonlinear optical material. *Mater. Chem. Phys.* **192**, 215–227 (2017)
 35. F. Urbach, The long-wavelength edge of photographic sensitivity and of the electronic absorption of solids. *Phys. Rev.* **92**, 1324 (1953)
 36. N.R. Rajagopalan, P. Krishnamoorthy, A systematic approach to physico-chemical analysis of tris (thiourea) zinc selenate – a semi-organic nonlinear optical crystal. *Optik* **129**, 118–129 (2017)
 37. M.C. Portillo, X. Mathew, H.J. Santiesteban, M.P. Castillo, O.P. Moreno, Growth and characterization of nanocrystalline PbS: Li thin films. *Superlattices Microstruc.* **98**, 242–252 (2016)
 38. F. Sevim, F. Demir, M. Bilen, H. Okur, Kinetic analysis of thermal decomposition of boric acid from thermogravimetric data. *Korean J. Chem. Eng.* **23**(5), 734–738 (2006)
 39. M. Lydia Caroline, G. Mani, S. Usha, Effect of Co²⁺ on the growth, optical properties and laser damage threshold of potential nonlinear optical L-alanine single crystal. *Optik* **125**, 5069–5074 (2016)
 40. Dursun Ali Köse, Michael A. Beckett, Naki Çolak, Synthesis, Spectroscopic and Thermal Characterization of Non-Metal Cation (NMC)Pentaborates Salts Containing Cations Derived From Histidine and Arginine. *J. Biol. & Chem.* **40**(3), 219–225 (2012)
 41. A. Darlin Mary, K. Jayakumari, C.K. Mahadevan, Growth and characterization of zinc magnesium tris (thiourea) sulphate (ZMTS) single crystals. *Int. J. Eng. Res. Appl.* **3**, 1183–1196 (2013)
 42. J.H. Joshi, S. Kalainathan, D.K. Kanchan, M.J. Joshi, K.D. Parikh, Effect of L-threonine on growth and properties of ammonium dihydrogen phosphate crystal. *Arab. J. Chem.* (2017). <https://doi.org/10.1016/j.arabjc.2017.12.005>
 43. J.H. Joshi, S. Kalainathan, M.J. Joshi, K.D. Parikh, Influence of L-serine on microstructural, spectroscopic, electrical and nonlinear optical performance of ammonium dihydrogen phosphate single crystal. *J. Mater. Sci.: Mater.* **30**, 14243–14255 (2019). <https://doi.org/10.1007/s10854-019-01793-0>
 44. E.M. Onitsch, The present status of testing the hardness of materials. *Mikroskopie* **95**, 12–14 (1956)
 45. B. Deepa, P. Philominathan, Investigation on the optical, mechanical and magnetic properties of organic NLO single crystal: Pyridine 3-carboxylic acid. *Optik* **127**, 8698–8705 (2016)
 46. K. Naseema, SarathRavi, RakhiSreedharan, Studies on a novel organic NLO single crystal: L-asparaginium Oxalate. *Chin. J. Phys.* **60**, 612–622 (2019)
 47. C. Rathika Thaya Kumari, P. Jayaprakash, M. Nageshwari, M. Peer Mohamed, P. Sangeetha, M. Lydia Caroline, Growth, optical, photoluminescence, dielectric, second and third order nonlinear optical studies of benzoyl valine acentric crystal. *Mol. Cryst. Liq. Cryst.* **658**, 186–197 (2017)
 48. H.J. Ravindra, A. JohnKiran, C.S.R. Nooji, S.M. Dharmaprakash, K. Chandrasekharan, Balakrishna Kalluraya, Fabian Rotermund, *J. Cryst. Growth* **310**, 2543–2549 (2008)
 49. K. Senthil, S. Kalainathan, F. Hamada, M. Yamada, P.G. Aravindan, Synthesis, growth, structural and HOMO and LUMO, MEP analysis of a new stilbazolium derivative crystal: A enhanced third-order NLO properties with a high laser-induced damage threshold for NLO applications. *Optical Mater.* **46**, 565–577 (2015)
 50. Z. Sun, G. Zhang, X. Wang, Z. Gao, X. Cheng, S. Zhang, D. Xu, Growth, Morphology, Thermal, Spectral, Linear, and Nonlinear Optical Properties of L-Arginine Bis(trifluoroacetate) Crystal. *Cryst. Growth Des.* **9**(7), 3251–3259 (2009)
 51. D.J. Daniel, P. Ramasamy, Studies on semi-organic nonlinear optical single crystal: Lithium formate monohydrate. *Opt. Mater.* **36**, 971–976 (2014)
 52. M. Lydia Caroline, S. Vasudevan, Growth and characterization of pure and doped bis thiourea zinc acetate: Semiorganic nonlinear optical single crystals. *Curr. Appl. Phys.* **9**(5), 1054–1061 (2009)
 53. M. Nageshwari, P. Jayaprakash, C.R.T. Kumari, G. Vinitha, M. Lydia Caroline, Growth, spectral, linear and nonlinear optical characteristics of an efficient semiorganic acentric crystal: L-Valinium L-Valine chloride. *Physics B* **511**, 1–9 (2017)
 54. N. Vijayan, K.R. Bhagavannarayana, R. Ramesh, R. Gopalakrishnan, K.K. Maurya, P. Ramasamy, A comparative study on solution and Bridgman grown single crystals of benzimidazole by high resolution X-ray diffractometry, fourier transform infrared, microhardness, laser damage

- threshold, and second harmonic generation measurements. *Cryst. Growth Des.* **6**, 1542–1546 (2006)
55. N.L. Boling, M.D. Crisp, G. Dube, Laser induced surface damage. *Appl. Opt.* **12**, 650–660 (1973)
 56. J.H. Joshi, D.K. Kanchan, M.J. Joshi, H.O. Jethva, K.D. Parikh, Dielectric relaxation, complex impedance and modulus spectroscopic studies of mix phase rod like cobalt sulfide nanoparticles. *Mater. Res. Bull.* **93**, 63–73 (2017)
 57. A.K. Jonscher, *Nature* **267**, 673 (1977)
 58. F.A. Najar, G.B. Vakil, B. Want, Structural, optical and dielectric studies of lithium sulphate monohydrate single crystals. *Mater. Sci. -Poland* (2017). <https://doi.org/10.1515/msp-2017-0002>
 59. K. Senthil, S. Kalainathan, A. Ruban Kumar, P.G. Aravindan, Investigation of synthesis, crystal structure and third order NLO properties of a new stilbazolium derivative crystal: a promising material for nonlinear optical devices. *RSC Adv.* **4**, 56112–27 (2014)
 60. P. Jayaprakash, M. Peer Mohamed, M. Lydia Caroline, Growth, spectral and optical characterization of a novel nonlinear optical organic material: D-Alanine DL-Mandelic acid single crystal. *Journal of Molecular Structure* **1134**, 67e77 (2017)
 61. C. Balarew, R. Duhlev, *J. Solid State Chem* **55**, 1–6 (1984)
 62. SK.Kurtz, T.A.Perry, *J.Appl.Phys* **39**, 3798–3813 (1968).
 63. T. Thilak, M. Basheer Ahamed, G. Vinitha, Third order nonlinear optical properties of potassium dichromate single crystals by Z-scan technique. *Optik* **124**, 4716–4720 (2013)
 64. M. Divya, P. Malliga, R. Divya, G. Vinitha, A. Joseph Arul Pragasam, Studies on third order nonlinear optical properties of Nickel Boro Phthalate NLO crystal. *Materials Research Express.* **6**, 11 (2019). <https://doi.org/10.1088/2053-1591/ab4d6d>
 65. P. Nagapandiselvi, C. Baby, R. Gopalakrishnan, Self-assembled supramolecular structure of N, N, N', N'- tetramethylethylenediammonium-bis-(4-nitrophenolate):synthesis, single crystal growth and photo physical properties. *RSC Adv.* **4**, 22350–22358 (2014)
 66. Y.S. Zhou, E.B. Wang, J. Peng, J. Liu, C.W. Hu, R.D. Huang, X. You, Synthesis and the third-order optical nonlinearities of two novel charge-transfer complexes of a heteropoly blue type (C₉H₇NO)₄ H₇PMo₁₂O₄₀·3H₂O (C₉H₇NO = quino-*lin*-8-ol) and (phen)₃ H₇PMo₁₂O₄₀·CH₃CN·H₂O (phen = 1,10-phenanthroline). *Polyhedron* **18**(10), 1419–1423 (1999). [https://doi.org/10.1016/S0277-5387\(98\)00448-3](https://doi.org/10.1016/S0277-5387(98)00448-3)
 67. W. Feng, W. Yi, H. Wu, M. Ozaki, K. Yoshino, Enhancement of third-order optical nonlinearities by conjugated polymer-bonded carbon nanotubes. *J. Appl. Phys.* **98**(3), 034301 (2005)
 68. V. Kannan, S. Brahadeeswaran, Synthesis, growth, thermal, optical and mechanical studies on 2-amino-6-methylpyridinium 4-hydroxybenzoate. *J. Therm. Anal. Calorim.* **124**, 2 (2016)
 69. V. Parol, A.N. Prabhu, M.A. Taher, S.R.G. Naraharisetty, N.K. Lokanath, A third-order nonlinear optical single crystal of 3, 4-dimethoxy-substituted chalcone derivative with high laser damage threshold value: a potential material for optical power. *J. Mater. Sci.: Mater. Electron.* **31**, 9133–9150 (2020)
 70. M.K. Kumar, S. Sudhahar, P. Pandi, G. Bhagavannaranya, R.M. Kumar, Studies of the structural and third-order nonlinear optical properties of solution grown 4-hydroxy-3-methoxy-4-N-methylstilbazoliumtosylate monohydrate crystals. *Opt. Mater.* **36**, 988 (2014)
 71. E. Raju, P. Jayaprakash, R. Ravisankar, M. Lydia Caroline, G. Vinitha, S. Kumaresan, Investigations on synthesis, growth and physicochemical properties of organic nonlinear optical crystal: 2-aminopyridinium maleate. *Inorg. Nano-Met. Chem.* (2022). <https://doi.org/10.1080/24701556.2022.206859>
 72. M. Dhavamurthy, R. Raja, K. SyedSuresh Babu, R. Mohan, Crystal structure, growth and characterization of a novel organic third-order nonlinear optical crystal: guanidinium cinnamate. *Appl. Phys. A.* **122**, 1–9 (2016). <https://doi.org/10.1007/s00339-016-0219-0>
 73. D. Wang, T. Li, S. Wang, Z. Wang, X. Xu, F. Zhang, Study on nonlinear refractive properties of KDP and DKDP crystals. *RSC Adv.* **6**(18), 14490–14495 (2016)
- Publisher's Note** Springer Nature remains neutral with regard to jurisdictional claims in published maps and institutional affiliations.
- Springer Nature or its licensor (e.g. a society or other partner) holds exclusive rights to this article under a publishing agreement with the author(s) or other rightsholder(s); author self-archiving of the accepted manuscript version of this article is solely governed by the terms of such publishing agreement and applicable law.